ISSN: 2155-6210

Journal of Biosensors & Bioelectronics

The International Open Access Journal of Biosensors & Bioelectronics

Available online at: OMICS Publishing Group (www.omicsonline.org)

Digital Object Identifier: http://dx.doi.org/10.4172/2155-6210.1000155

Biosensors & Bioelectronics

Peeters et al., J Biosens Bioelectron 2014, 5:3
http://dx.doi.org/10.4172/2155-6210.1000155

Research Article Open Access

Real-Time Monitoring of Aptamer Functionalization and Detection of Ara H1 by Electrochemical Impedance Spectroscopy and Dissipation-Mode Quartz Crystal Microbalance

Peeters M[1,2,*], Jiménez-Monroy K[1], Libert C[1], Eurlings Y[1], Cuypers W[1], Wackers G[1], Duchateau S[1], Robaeys P[1], Nesládek M[1,2], van Grinsven B[1,3], Pérez-Ruiz E[4], Lammertyn J[4], Losada-Pérez P[1,2] and Wagner P[1,2]

[1]*Institute for Materials Research, Hasselt University, Wetenschapspark 1, 3590 Diepenbeek, Belgium*
[2]*IMEC vzw, division IMOMEC, Wetenschapspark 1, 3590 Diepenbeek, Belgium*
[3]*Maastricht University, Maastricht Science Programme, Maastricht, The Netherlands*
[4]*BIOSYST-MeBioS, KU Leuven – University of Leuven, Willem de Crooylaan 42, 3000 Leuven, Belgium*

Abstract

Peanut allergy, the most common cause of fatal-food-related anaphylaxis, is a lifelong disorder and the only existing therapy is avoidance of allergen-containing food. Detection of Ara h 1, the most important peanut allergen, is commonly performed by immunoassay techniques relying on the use of expensive and relatively unstable antibodies. Aptamers can overcome these drawbacks and offer a great potential for the development of reliable biosensors. Therefore, we will present a novel aptamer-based sensor for the label-free detection of Ara h 1. Amino (NH_2)-terminated Ara h 1 aptamers were covalently attached to carboxylated gold surfaces employing carbodiimide chemistry. This functionalization procedure was followed *in real time* by electrochemical impedance spectroscopy and quartz crystal microbalance with dissipation monitoring. Subsequently, the functionalized surfaces were exposed to Ara h 1 solutions in TGK buffer. By combining the two techniques, we can measure in a wide concentration regime varying from the low nanomolar range (1-15 nM) via electrochemical impedance spectroscopy to the higher concentrations (25-250 nM) by microgravimetric detection. In summary, a fast, low-cost and sensitive sensor platform for Ara h 1 detection has been developed, which can be operated as a 'stand-alone device', making it well suited for applications such as the screening of trace allergens.

Keywords: Aptamers; Biosensors; Quartz crystal microbalance; Electrochemical impedance spectroscopy; Atomic force microscopy; Ara h 1; Peanut allergy

Introduction

Peanut allergy affects about 1% of the total population worldwide and is the most common cause of fatal-food-related anaphylaxis [1]. It is a lifelong disorder with a high risk of accidental exposure [2]. Low milligram amounts of peanut allergens can induce severe allergic reactions, and much attention has been paid to the detection of immunogenic proteins present in peanuts since no cure is available [3,4]. Ara h 1, a homotrimeric protein with a molecular weight of 65 kDa, is abundantly present in peanuts and is shown to account for almost 95% of all peanut-allergenicity reactions [5,6]. It forms a highly stable trimer of which all epitopes are harbored in a hydrophobic region, secluded from digestive enzymes [7,8]. This protects the allergen from proteolytic digestion in the gastrointestinal tract. Furthermore, during cooking of food its allergenicity is unaffected by heating [6], meaning it can still trigger an immunogenic response after preparation [9]. To date, several immunoassays have been described in literature for detection of this allergen including Enzyme Linked Immuno-Sorbent Assay (ELISA) [10], lateral flow assay [11], immune sensors and mass spectroscopy [12-14]. They rely on the detection by antibodies which are expensive and possess a limited working range and shelf life [15]. In contrast, aptamers, single stranded DNA (ssDNA) or RNA oligonucleotides that can specifically bind a target molecule are smaller, less expensive, and more stable while still having similar affinity to their target molecules as compared to natural antibodies [16-18]. Aptamers can be selected against a variety of targets with a molecular selection process known as Systematic Evolution of Ligands by exponential enrichment (SELEX) [19,20]. In previous work [21], determined the best performing Ara h 1 DNA aptamer by combining SELEX with Capillary Electrophoresis (CE). Subsequently, dissociation constants were obtained by three independent techniques; surface plasmon resonance (353 ± 82 nM), fluorescence anisotropy (419 ± 63 nM), and capillary electrophoresis (450 ± 60 nM). Recently, dissociation kinetics of the bonds between the aptamer and Ara h 1 were also studied with magnetic force-induced dissociation approach [22]. An interesting alternative is impedance spectroscopy, which has been applied previously for IgE detection with a diamond sensing platform [21]. In that contribution, measurements were performed with a sophisticated commercial impedance analyzer, which requires a long measurement time. Recently, new home-made setups have been developed which are low-cost and can perform fast measurements [23-25]. The duration of one frequency sweep from 100 Hz to 100 kHz is reduced to several seconds and, in addition, only limited hardware is required. In this article, we report on real-time impedimetric sensing of peanut allergens by using gold substrates functionalized with aptamer receptors against Ara h 1. As a validation technique, the Quartz Crystal Microbalance with dissipation monitoring (QCM-D) will be employed. The functionalization method is a two-step procedure and consists of forming a Self-Assembled Monolayer (SAM) of thiols followed by the covalent binding of the amine modified aptamer via directed EDC coupling [26,27]. To reduce non-specific binding, the remaining part of the surface is blocked by immersing it into a Bovine Serum Albumin (BSA) solution. After this step, the aptasensor is ready for use (Figure S-1). We will demonstrate that the dynamic range of the sensor platform with impedance spectroscopy as read-out technique is in the lower nanomolar regime (3-40 nM) while with the microgravimetric method (QCM-D) higher concentrations (25-250 nM) can be measured. Results are obtained within 15 min and with fully home-made equipment in the case of

***Corresponding author:** Marloes Peeters, 1Institute for Materials Research, Hasselt University, Wetenschapspark, Belgium, Tel: +32-11-26-8876; Fax: +32-11-26-8899; E-mail: marloes.peeters@uhasselt.be

Received June 20, 2014; **Accepted** July 14, 2014; **Published** July 21, 2014

Citation: Peeters M, Jiménez-Monroy K, Libert C, Eurlings Y, Cuypers W, et al. (2014) Real-Time Monitoring of Aptamer Functionalization and Detection of Ara H 1 by Electrochemical Impedance Spectroscopy and Dissipation-Mode Quartz Crystal Microbalance. J Biosens Bioelectron 5: 155. doi: 10.4172/2155-6210.1000155

impedance spectroscopy. Reference experiments are conducted with proteins similar in molecular weight as Ara h 1 to address the selectivity of the sensor platform. An additional advantage of this method is that it can be extended to other important protein markers. In summary, a fast, low-cost, and sensitive bioassay has been developed which has the potential to be applied for the screening of trace allergens.

Materials and Methods

Materials

The allergen, Ara h 1, was purchased from INDOOR biotechnologies (Cardiff, Wales) and used as received. The aptamer was obtained from IDT technologies (Leuven, Belgium) and had the following 80 base pairs sequence:

5'TCGCACATTCCGCTTCTACCGGGGGGGTCGAGCGAGT-GAGC GAATCTGTGGGTGGGCCGTAAGTCCGTGTGTG CGAA 3'

The 5'end was modified with an amino group and a C_6 carbon spacer.

The QCM-D quartz crystals, coated with Au, were obtained from Q-sense. 1-ethyl-3-(3-dimethylaminopropyl) (EDC) was purchased from Thermo Scientific (Aalst, Belgium), 11-mercapto-undecanoic acid (95%), horse radish peroxidase (M_r ~ 40 kDa, HRP) and bovine serum albumin (M_r ~66.5 kDa, BSA) from Sigma Aldrich (Steinheim, Germany). All compounds used for the preparation of the buffers, 2-(N-morpholino)ethanesulfonic acid (MES) buffer, tris(hydroxyamino)methane-glycine-potassium (TGK) buffer and PBS buffer, were obtained from commercial resources (Sigma Aldrich and Fisher Scientific) and were of highest purity. Ethanol (anhydrous, 99.9%) was of analytical grade. Buffers were adjusted to the right pH by addition of Hydrochloric Acid (HCl) and sodium hydroxide (NaOH) solutions in MilliQ water.

Atomic force microscopy

Atomic Force Microscopy (AFM) was carried out to characterize the aptamer biosensing layer. The Au-coated QCM substrates or the silicon substrates with gold deposited on it could not be employed since their roughness was too high; therefore, the aptamer was adsorbed onto an ultra-flat Muscovite mica surface (0.15-0.21 mm thickness, Electron Microscopy Sciences, USA). The substrate root mean squared roughness (RMS) was 0.08 nm (Figure S-2). Subsequently, the layer thickness and height were evaluated with a NX10 AFM instrument (Park Instruments, Korea) in non-contact mode. A standard pyramidal shaped Si_3N_4 (silicon nitride) cantilever with a length of 125 nm and a nominal force constant of 40 N/m was used. The measurements were performed in air at room temperature and the dimensions were compared to theoretical calculations based on the online software package Mfold from University at Albany (New York, United States) [28,29].

QCM-D measurements

QCM-D measurements were performed on a Q-sense E4 instrument (Gothenborg, Sweden). This device monitors the changes in resonance frequency (Δf) and in dissipation (ΔD), which provides information on the adsorbed mass on the solid support and on the viscoelastic properties of the adsorbed layer. AT-cut quartz crystals with Au coating (diameter 14 mm, thickness 0.3 mm, surface roughness 3 nm and resonance frequency 4.95 MHz) were employed. These were cleaned with a 5: 1: 1: mixture of MilliQ-water, ammonia and hydrogen peroxide followed by a second cleaning step with isopropanol. Prior to formation of the SAM-layer, the crystals were treated with a Digital PSD series UV-ozone system from Novoscan for 1h.

With the QCM-D, both the functionalization of the surface and the subsequent detection of Ara h 1 can be monitored *in situ.* The system was operated under flow conditions with a constant flow rate of 200 µL/min. The chamber temperature was set at 37.00°C and the changes in Δf and ΔD were recorded at five different overtones (from 3rd to 11th). The harmonic frequency was omitted because of stability purposes. For the formation of the self-assembled monolayer, the system was first flushed with ethanol in order to establish a baseline. Subsequently, the crystals were exposed to a solution of 11-mercapto-undecanoic acid (1 mM) in ethanol. After stabilization, the coupling was performed by introducing a solution of EDC (400 mM) and aptamer (0.1µM) in a MES buffer with pH 6. The crystals were then taken out of the chambers and immersed into a 100 nM BSA solution in PBS in order to reduce non-specific binding on the sensor surface. Aptamers have a very high stability and can even circulate in human blood plasma for weeks without being denatured. This means that after functionalization the sensor can be stored for several weeks until sensing experiments will be performed. The final step, the recognition of Ara h 1, was done in a specific TGK buffer at pH 8.3 as was recommended in previous work. The TGK buffer was first introduced into the flow chamber, followed by addition of increasing allergen concentrations (37.5, 75, 150, 225 and 750 nM) in buffer.

Impedance spectroscopy measurements

The employed impedance spectroscopy unit is an in-house design which is described in detail [30] . Impedance data were recorded from 100 Hz to 100 kHz, built up logarithmically with 10 frequencies per decade, with a full frequency sweep taking 5.4s in total. The system was coupled to a Perspex flow cell with an internal volume of 110 µl onto which samples were mounted horizontally. A gold wire (diameter 500 mm) at a distance of 1.7 mm from the sensor surface was used as a counter electrode. The working electrode was pressed onto a copper lid, serving as a back electrode as well as heat sink. Miniaturized thermocouples were integrated in the heat sink and in the liquid (Figure 1). In previous research, this flow-through measurement sensor cell has been used for the electronic detection of serotonin in human blood plasma and of histamine in bowel fluid by MIP-type receptors [31,32].

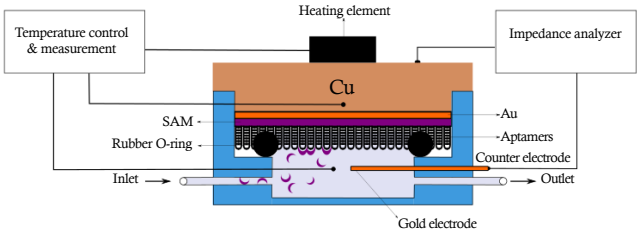

Figure 1: Schematic layout of the measurement setup, allowing the detection of Ara h 1 (represented by semicircles) by the aptamer functionalized on a gold substrate (1x1 cm2). The cell, with an inner volume of 110 µl, was filled with TGK buffer and a thermocouple was used to measure the temperature of the copper which was stabilized at 37.00° C using a PID-controller (P= 1, I= 8, D= 0.1). The impedance was monitored through the copper to the counter electrode in the liquid at 1.7 mm of the sensor surface. This configuration prevented sedimentation of molecules onto the sensor surface, thereby reducing non-specific binding.

The functionalization protocol of the gold surface was similar to that of the QCM-D measurements and after each step, Nyquist plots were measured. Gold electrodes were prepared as follows; metal evaporation onto doped silicon substrates was performed at 5×10^{-5} Pa. First, 20 nm of chromium was deposited onto the substrates on top of which a 80 nm thick gold layer was evaporated. These substrates (1x1 cm^2) were treated with a Digital PSD series UV-ozone system from Novoscan for 1 h. Then, they were cleaned by dipping them into a cold "piranha" solution (H_2O_2: H_2SO_4 1: 3) followed by rinsing with ethanol. An 11-mercapto-undecanoic acid solution in ethanol (1 mM) was applied onto the surface and the substrate was incubated under nitrogen atmosphere for 48 h. After washing with ethanol, the aptamer was attached via directed EDC coupling in MES buffer of pH 6 which was monitored *in-situ*. Finally, to reduce non-specific binding, the aptamer-coated gold substrates were immersed overnight into in a 100 nM BSA solution in PBS buffer.

The aptasensor was now ready to use for experiments. First, the sensor measurement chamber was filled with TGK buffer of pH 8.3 and left to stabilize for 30 min. After this period, solutions of increasing concentrations Ara h 1 (3.33 to 50 nM) in TGK buffer were introduced resulting in an increase in the impedance. To check whether the allergen was firmly attached to the aptamer, a flushing step with buffer was performed. In order to address the selectivity of the platform, reference experiments were conducted with BSA and HRP and also the attachment of the allergen to a substrate solely functionalized with SAM and no aptamer was analyzed.

Results and Discussion

AFM studies

Measurements were performed in air at room temperature. Five microliters of the aptamer and allergen solution in demineralized water (0.1 μM) were deposited on top of freshly cleaved mica substrate and placed on a desiccator for 1 h. Afterwards, the configurations were studied under the AFM. Since both structures can adopt different conformations in the dry state, different molecules were studied and its most representative structures were evaluated. It is known that the aptamer has a circular structure and, for a section of worm-like coil of contour length, the Flory radius (R_f) is determined with the following formula [33]:

$$R_f^2 = 2 \times L_p \times L\left[\left(1-\frac{L_p}{L}\left(1-e^{-\left(L/L_p\right)}\right)\right)\right]$$

Where L, the length of the ss DNA strand, is defined as L=N x l, with N being the number of nucleotides and l is the length of each nucleotide. With L_p, the persistence length, equal to two base pairs, N is 80 nucleotides and l is 0.7 nm, a Flory radius of 14.7 nm is obtained. The diameter of the aptamer would then be 29.4 nm and can be compared to what is obtained by AFM as shown in Figure 2a. In Figure 2b, the structure of the allergen Ara h 1 was analysed which was deposited onto the mica substrate in the same manner as for the aptamer. The aptamer configuration can also be modelled with online available Mfold software which calculates the most likely secondary structures of the aptamer according to the laws of thermodynamics. This was done at 20°C and 37°C in order to study the optimal temperature configuration (Figure 2c and Figure 2d).

By AFM (Figure 2a), the aptamer dimensions were determined and the length was 29.3 nm with a height of 2.5 nm. This is comparable to what was obtained by theoretical calculations (D=29.4 nm) and confirms attachment of the aptamer to the surface. The AFM image of the allergen Ara h 1 gave insight into its molecular conformation (Figure 2b). The volume of the protein molecule was calculated theoretically according to partial specific volumes and densities taken from literature [34]. To match theoretical and experimentally obtained results, the allergen has to be in the more stable trimer state which resulted in a diameter of ~11 nm and this was well in accordance with the AFM results (~13.3 nm). In further experiments, the molecular weight of the trimer Ara h 1 will be used to determine the concentrations.

In Figure 2c and d the most likely secondary structures, according to Mfold software, are presented at two different temperatures. There are multiple options, but all of them contain the internal loops with constant regions which are known to be involved in the recognition of Ara h 1 [21]. In the case of 20°C, the structure is more extended and the recognition sites are further apart which could have an adverse effect on the binding of Ara h 1. This will be experimentally verified by QCM-D measurements which will be described in Section 3.2.

QCM-D measurements

The first step of the functionalization procedure, the formation of a SAM on the gold surface, was monitored *in real time* by QCM-D. It was carried out at 37.00°C with different concentrations of 11-mercapto-undecanoic acid (10 mM, 2 mM, 1mM) in ethanol. The results of the normalized frequency and dissipation, respectively Δf/n and ΔD, are shown with a thiol concentration of 10 mM since it yielded the highest response (Figure 3a). During the measurement, the flow rate was kept constant at 200 μL/min.

Figure 3a shows that, when the thiol solution was added, the frequency decreased rapidly while the dissipation increased. A stable plateau was reached at -16 Hz and 4.7×10^{-6} at the 9th overtone. While this proves that the SAM formation can be monitored at high concentrations, the response in frequency is only minor because the layer is very thin (several nanometers). To ascertain a monolayer will be used, in further experiments a low thiol concentration of 1 mM will be employed, which is similar to previous reports in literature [21].

After formation of the SAM, the gold crystals were stabilized in MES buffer of pH 6. Then, a solution containing EDC (400 mM) and aptamer (0.1μM) was introduced into the system. The results on the frequency and the differential dissipation at the 9th overtone are shown in Figure 3B. The other overtones are not given since they overlap for both the normalized frequency and of the dissipation with the 9th overtone. After the EDC/aptamer mixture was injected, it takes 5 min for the solution to reach the surface and start the reaction. The coupling is finalized within 20 min since after that time no significant effect on the frequency and the dissipation is observed anymore. As a result, the frequency decreased with -8.5 Hz and the dissipation increases by 0.88×10^{-6} at the 9th overtone demonstrating the attachment of the aptamer. After this procedure, the crystals were immersed into a BSA solution (100 nM in 1x PBS). In the final step, the aptamer-coated gold crystals are stabilized in TGK buffer at 37.00°C and exposed sequentially to increasing concentrations of Ara h 1 (12.5, 25, 50, 75, 250 nM) in TGK buffer at a flow rate of 200 μL/min. In between the additions of the peanut allergen, flushing steps with protein-free TGK buffer were performed until a stable plateau level was reached. When the signal stabilized again, a new concentration of Ara h 1 was introduced. The results on the differential frequency and dissipation at the 9th overtone are shown in Figures 4a. This overtone was selected due to its higher stability. The corresponding dose-response, based on the frequency results, is depicted in Figure 4b.

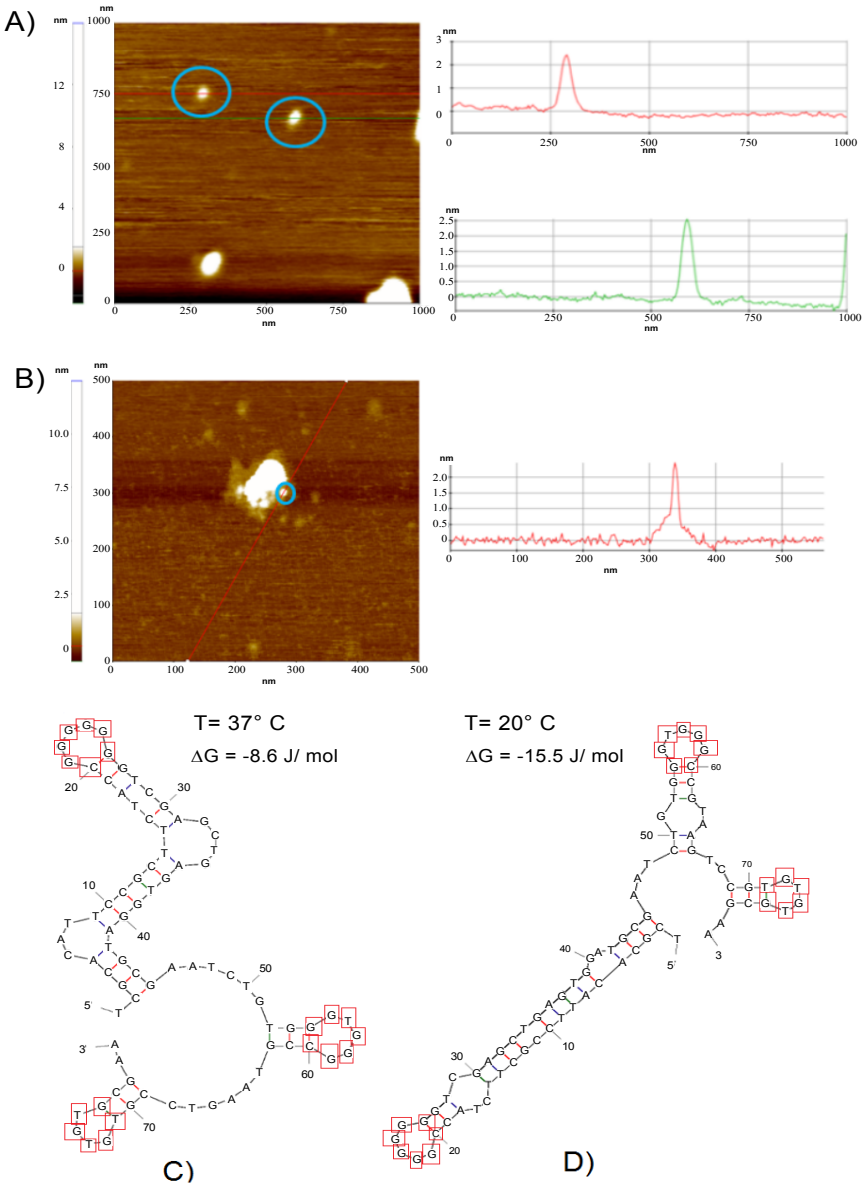

Figure 2: a) AFM image scan size was of 1 x 1µm2. Red and green line profiles show two aptamers (circled in blue, for guide of the eye) of 29.3 nm length and 2.5 nm height. B) AFM image of the allergen Ara h 1. Out of the agglomerate, the allergen was determined with a length of 13 nm length and 2.5 when the scan size was reduced to 0.5 x0.5 µm2. c) The most likely secondary structure of the aptamer as calculated by Mfold software are given. It shows that the configuration at 37°C (ΔG = -8.6 J/mol) is is more compact as compared to d) at 20°C (ΔG = -15.5 J/mol).

Upon exposure of the sensor to a 12.5 nM Ara h 1 concentration in TGK buffer, no significant effect in the frequency or the dissipation is observed. Starting from 37.5 nM, binding to the aptamer functionalized surface can be detected and the frequency decreases depending on the Ara h 1 concentration with a maximum difference of 68.3 ± 0.2 Hz (Figure 4a). In the dissipation, the effect is less pronounced and initially some drift on the signal is observed. However, concentrations of 50 nM or higher result in a dissipation increase with a maximum of 4.7 ± 0.1×10^{-6} (Figure 4a). To determine the exact allergen concentrations, a dose-response curve can be constructed which correlates the effect size to the corresponding Ara h 1 concentration in TGK buffer. This was done with the frequency since it yielded clearer responses than in the dissipation (Figure 4b). The overtones overlap and exhibit the same response, for stability purposes the 9th harmonic overtone was selected for obtaining the dose-response curve. These results can also be modeled very well (R^2=0.99) according to a typical sigmoidal dose-response curve with the following equation [35]:

$$y = A_1 + (A_2 - A_1) / (1 + 10\text{^}((LogEC50 - c) \times p)).$$

In this formula, y is the frequency response (Hz), A_1 the y-value of the lower plateau, A_2 is the y-value of the top plateau, log EC50 is the x-value where the inflection point of the curve is, x corresponds to the

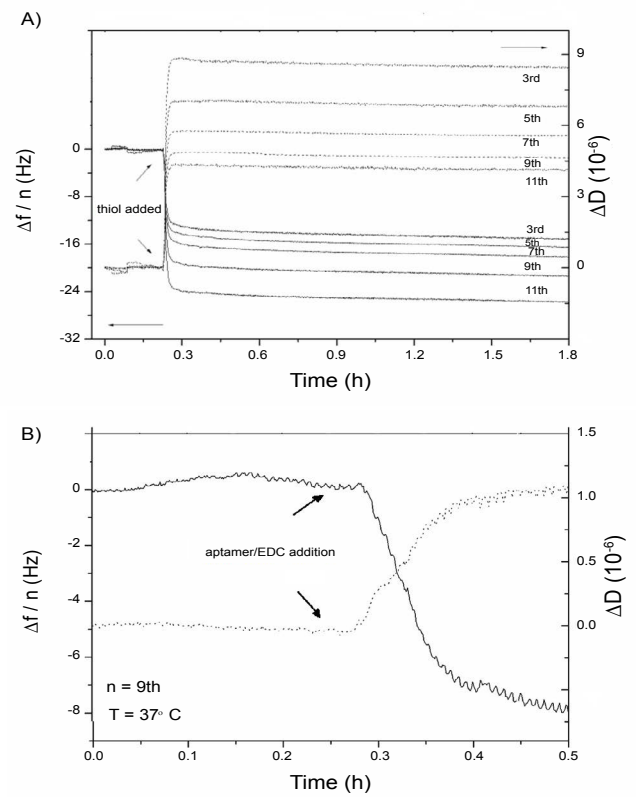

Figure 3: a) Time evolution of the normalized frequency (Δf/n) (solid lines) and ΔD (dashed lines) during SAM formation b) Time evolution of the change in frequency (solid line) and ΔD (dashed line) at the 9th overtone during aptamer attachment via EDC coupling. For both experiments, the temperature was stabilized at 37.00 °C and the system was operated under flow conditions (rate 200 µL/min).

Ara h 1 concentration (nM), and p is the Hill slope which describes the steepness of the curve. These parameters are given in Table S-1.The dynamic range of the QCM-based sensor is from 25 to 250 nM with a sensitivity of 0.30 Hz/nM. When the overtones overlap, the Sauerbrey equation can be applied and the mass deposited on the surface can be calculated according to:

$$\Delta m = \Delta f/n \times c$$

In this equation, Δm corresponds to the mass difference (ng), Δf / n to the normalized differential frequency (Hz), and c is a constant of 17.7 ng/Hz for a 4.95 MHz Au-coated quartz crystal, as determined by the manufacturer or the crystals Q-Sense (Gothenborg, Sweden). With these values, we obtain that the lowest amount of mass that can be detected on the sensor is surface is 123.9 ng and the maximum equals 1208.9 ng.

This, however, does not verify whether the surface was sufficiently blocked in order to reduce non-specific binding to the sensor surface. Therefore, experiments were conducted by exposing the fully functionalized crystals to BSA solutions in TGK buffer. The results, shown in Figure S-3, demonstrate that BSA does not bind to the aptasensor and therefore the blocking of the surface was successful and non-specific binding is reduced. A more stringent specificity test, exposing the aptasensor to a competitor protein, was performed with impedance spectroscopy experiments and will be described in Section 3.3.

Another parameter that was evaluated was the effect of the temperature. Using Mfold software, we determined that the more compact secondary structure at 37°C promotes binding which is experimentally verified by QCM-D, since this technique allows measurements to be performed in the 15 - 50°C range. Figure S-3 shows that at every concentration, the response at 37°C is higher compared to what was obtained at 20°C. At the highest concentration of 250 nM only a response of 46.6 ± 1.0 Hz was measured at 20°C, while at 37°C this was 68.3 ± 0.2 Hz (Figure S-4). Therefore, in further experiments with impedance spectroscopy the temperature was kept at 37°C since this was determined to be optimal.

Impedance spectroscopy results

Impedance spectroscopy does not allow for monitoring of the SAM formation *in real time* due to the use of the non-ionic solvent ethanol. However, Nyquists plots were recorded after the formation of a SAM on a gold substrate and subsequently after coupling of the aptamer to the surface. This was accomplished by mounting the gold substrates in the setup described in Section 2.3 and filling the flow cell with TGK buffer. The impedance data were measured from 100 Hz to 100 kHz at 37°C (Figure 5). In order to more precisely determine the effect of the different functionalization steps, the data was fitted ($\chi^2 \sim 1\times10^{-3}$) with a Randles circuit which only consists out of three parameters.

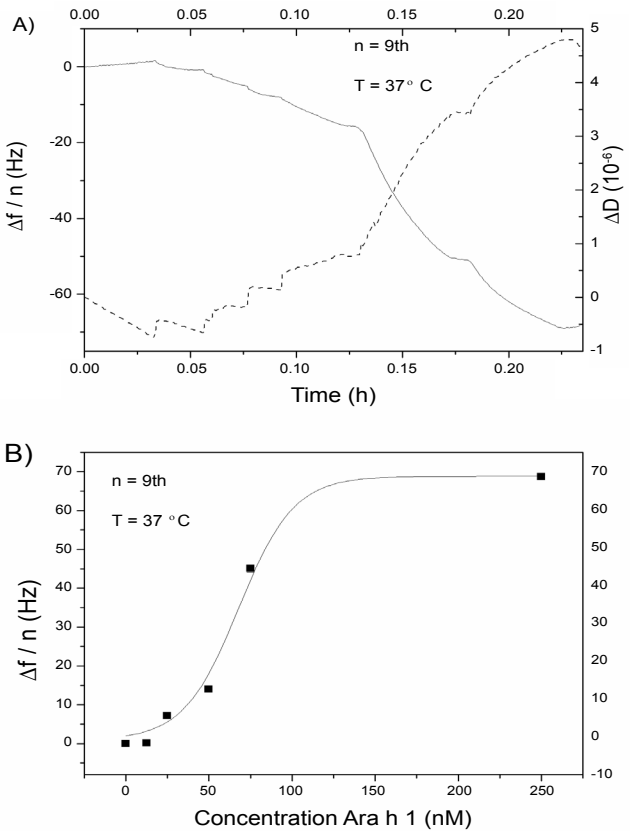

Figure 4: a) Response in the differential frequency, Δf/n and in ΔD upon exposure of increasing concentrations of Ara h 1 in TGK buffer. The fit, curve given as a solid line, corresponds to a typical sigmoidal plot with an R2 of 0.99. b) Dose-response curve constructed by plotting the concentration vs the response in frequency. All results shown belong to the 9th overtone and were obtained at T = 37.00°C. The error bars were calculated by averaging out the data over three separate measurements, but can be smaller than symbol size.

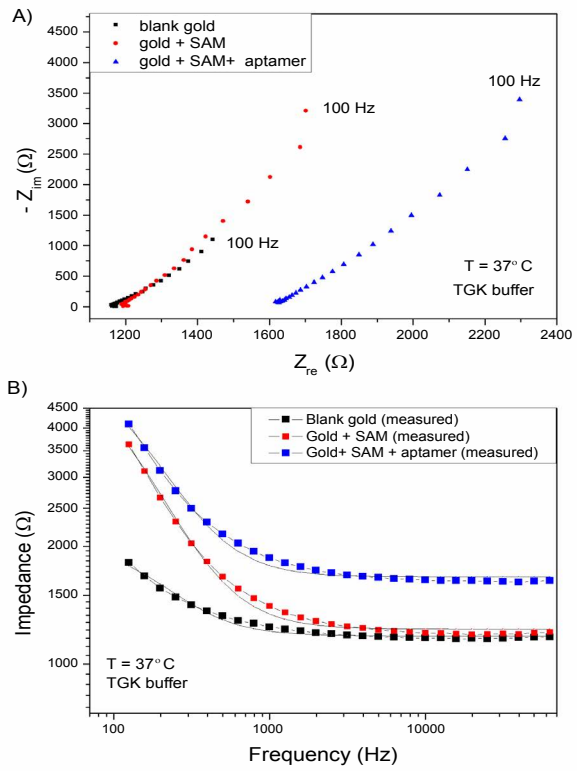

Figure 5: a) Nyquist plots obtained after measuring blank gold (black solid squares), the same sample modified with SAM (red solid circles) and followed by aptamer attachment (blue solid circles). b) This data was fitted with a three parameters equivalent circuit and the results of the measured (filled squares) and fitted (solid lines) impedance data are shown. The frequency and impedance are both plotted logarithmically. All measurements were performed in TGK buffer at 37°C.

From Figure 5, it is directly clear that after each functionalization step, significant changes in the Nyquist plots (Figure 5a) and the impedance data (Figure 5b) are observed. The effect of these changes can be studied if the data are fitted with a common three elements equivalent circuit, consisting of the solution-phase resistance in series with a capacitor that is in turn parallel with its corresponding resistance. In the first step, the capacitance is affected by forming the SAM layer while aptamer attachment resulted mainly in an increase of the charge-transfer resistance. The effect on the parameters of the three element circuit is given in Table S-2. These results corroborate the QCM-D data and, additionally, there is the option to monitor the aptamer attachment *in real time* since this occurs in MES buffer. These results, obtained after introducing an EDC/aptamer solution in MES buffer to a SAM coated gold substrate, are shown in Figure S-5. Prior to measuring of Ara h 1, the substrate was immersed into a BSA solution in PBS overnight in order to block the non-functionalized surface. It is mounted in the setup and left in TGK buffer at 37.0°C. When a stable baseline was reached, increasing concentrations of Ara h 1 (3.33, 6.67, 10, 15, 25 and 50 nM) were added. At the end, the flow cell was flushed with TGK in order to demonstrate firm attachment of the allergen to the aptamer. The results at a frequency of 316 Hz are shown in Figure 5a. Data were recorded in the entire regime, but at this particular frequency the signal-to-noise ratio was optimal. To construct the dose-response curve, we take the values after letting it stabilize for 10 min after addition and then dividing it over the impedance at base level to obtain the normalized response, which is the impedance at a certain concentration divided over the baseline level (Figure 6a). In order to determine the origin of the impedance increase, the system was modeled with a five parameters equivalent circuit model which is shown in Figure S-6. The three circuit equivalent parameter model which was used for the Nyquist plots for the functionalization procedure does not apply anymore and only gives a χ^2 value of 1×10^{-2}. This can be explained by the addition of the extra blocking BSA layer on the surface and the fact that the aptamer adopts a different conformation when the analyte Ara h 1 is bound. Therefore, the circuit consisting of five elements was employed which gave a more accurate description of the system and resulted in a χ^2 value of ~0.5×10^{-3}. When evaluating the effect on the different parameters of this equivalent circuit, as is shown in Table S-2, the most pronounced effect is observed in the charge-transfer resistance. This corroborates previous literature reports which describe that with higher protein concentrations, the charge-transfer resistance increases due to a thicker protein film thickness on the electrode [12]. The effect of the concentration Ara h 1 on R_{ct} is given in Figure 6b. This process is also illustrated by the Nyquist plots constructed during stabilization and after exposure to a 50 nM concentration of Ara h 1

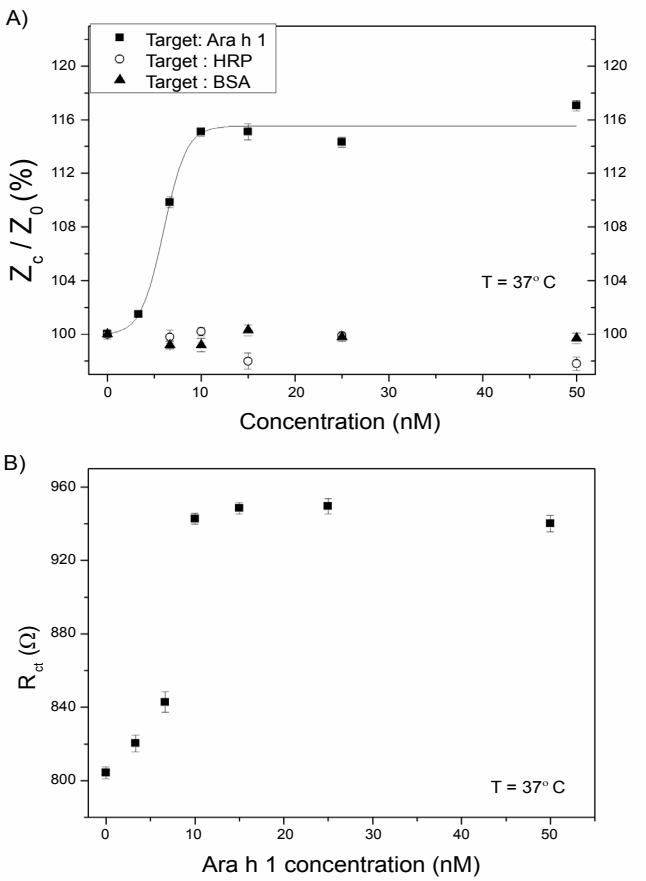

Figure 6: a) is the dose-response curve and shows the normalized response (Zc / Z0) at a frequency of 316 Hz (T = 37°C) when solutions of Ara h 1 in PBS (3.33, 6.67, 10, 15, 25, 50 nM) were introduced. As reference test, the same experiment was performed with the proteins HRP and BSA. The error bars were taken over three measurements which were performed independently with freshly prepared electrodes. The fit given for the Ara h1 concentration is a typical sigmoidal plot with a R2 of 0.98. b) demonstrates that the impedance increase mainly can be attributed to an increase in the charge transfer resistance Rct.

(Figure S-7). There is a clear shift along the x-direction, corresponding to an increase of the real part of the impedance.

Figure 6a demonstrates that the linear regime of the sensor platform is from 3.33-15 nM after which saturation is occurring. This corresponds well (R^2=0.98) to a typical sigmoidal dose-response curve, as was also observed in the QCM-results. The parameters for these fit are given in Table S-3.

Table S-4 shows that the increase in impedance can mainly be attributed to an increase in R_{ct}; therefore, the effect of the Ara h 1 concentration on R_{ct} is shown in Figure 6b. In the linear regime of the sensor platform (0-10 nM), the sensitivity was determined to be 1.3%/nM. With these data points, it also possible to estimate the detection limit. Generally, this is defined as the concentration at which the response is three times the noise on the base line level. In this case, it would be approximately 1 nM, demonstrating the excellent specificity of the developed sensor platform. Similar detection limits were obtained with immuno-assays such as ELISA, SPR, lateral flow assays, or impedimetric read-out . However, it has to be noted that with ELISA and SPR sophisticated equipment is required and for a low-cost and fast alternative, the lateral flow assay, only a yes/no response was obtained and not a quantitative result. The impedimetric approach was performed with a commercial analyzer compared to our described home-made setup and takes ~2.5 min for one frequency sweep while with the developed device only 5.4 s is needed. In addition, an experiment was conducted with BSA to evaluate if the surface was sufficiently blocked. Figure S-6 a shows no significant effect of the addition of protein concentrations (6.67-50 nM) in TGK, indicating non-specific binding is reduced. Afterwards another reference experiment was conducted, with the protein HRP, which has a similar molecular weight Ara h 1 and can therefore be considered an interesting competitor. In Figure S-6 b is shown that upon exposure to HRP, even at high concentrations of the protein (50 nM) no impedance response observed, demonstrating the selectivity of the sensor platform.

Conclusions

We have presented a novel aptamer-based sensor platform for the fast and label-free detection of peanut allergen Ara h 1. The sensor surface was functionalized with Ara h 1 aptamer via a simple two-step procedure; first, a SAM was formed with an acid functionality, and second, via directed EDC coupling amino-terminated Ara h 1 aptamers can be covalently attached to the carboxylated gold electrode. These processes were monitored *in real time* by QCM-D technology, demonstrating successful functionalization of the surface. After each functionalization step, the impedance spectra were measured and the differences in the parameters of the electrical equivalent three parameters circuit confirm the results obtained by QCM-D. With AFM, it was also determined that the aptamer was on the surface and its diameter was estimated to be 29.3 nm, which is in agreement with theoretical calculations on the Flory radius. Subsequently, the aptamer-coated gold surfaces were exposed to Ara h 1 concentrations in buffer solutions, and *in real-time* the detection was followed by electrochemical impedance spectroscopy and QCM-D. Both techniques show a fast response time with results that are obtained within several minutes. Addition of the allergen caused an increase in the impedance, which is attributed to the change in charge-transfer resistance due to the difference in film thickness. By monitoring this parameter, the sensor platform is especially sensitive in the low nanomolar regime and can detect Ara h1 with a detection limit of ~1 nM and up to concentrations of ~15 nM. Selectivity of the aptasensor was demonstrated by reference measurements with HRP, a protein with similar molecular weight as the peanut allergen. QCM-D has a higher detection limit and with this, read-out technique responses are obtained from ~25 nM to 250 nM. In summary, a fast, low-cost and sensitive sensor platform for Ara h 1 detection has been developed which can be operated as a 'stand-alone device'. Since the developed platform can measure in a wide concentration regime, it is well suited for applications such as the measurement of peanut-related food samples with QCM-based detection as well as the more sensitive screening of trace allergens by electrochemical impedance spectroscopy.

Acknowledgements

This work is supported by the FWO project G.0997.11N (M. Peeters and E. Pérez-Ruiz), the Life Science Initiative of the Belgian Province of Limburg and the European Commission's Seventh Framework Programme (FP7/2007-2013) under the grant agreement BIOMAX (Project No. 264737). The authors also would like to thank H. Penxten, J. Soogen, C. Willems, W. Stilman, J. Smits and J. Baccus for technical assistance. Prof. W. De Ceuninck is acknowledged for stimulating scientific discussions and K. Ranieri for assisting with textural support.

References

1. Sicherer SH, Sampson HA (2007) Peanut allergy: emerging concepts and approaches for an apparent epidemic. J Allergy Clin Immunol 120: 491-503.
2. Kleber-Janke T, Crameri R, Appenzeller U, Schlaak M, Becker WM (1999) Selective cloning of peanut allergens, including profilin and 2S albumins, by phage display technology. Int Arch Allergy Immunol 119: 265-274.
3. Poms RE, Agazzi ME, Bau A, Brohee M, Capelletti C, et al. (2005) Inter-laboratory validation study of five commercial ELISA test kits for the determination of peanut proteins in biscuits and dark chocolate. Food Addit Contam 22: 104-112.
4. Sampson HA (2003) Anaphylaxis and emergency treatment. Pediatrics 111: 1601-1608.
5. Burks AW, Williams LW, Helm RM, Connaughton C, Cockrell G, et al. (1991) Identification of a major peanut allergen, Ara h I, in patients with atopic dermatitis and positive peanut challenges. J Allergy Clin Immunol 88: 172-179.
6. Koppelman SJ, Wensing M, Ertmann M, Knulst AC, Knol EF (2004) Relevance of Ara h1, Ara h2 and Ara h3 in peanut-allergic patients, as determined by immunoglobulin E Western blotting, basophil-histamine release and intracutaneous testing: Ara h2 is the most important peanut allergen. Clin Exp Allergy 34: 583-590.
7. Sen M, Kopper R, Pons L, Abraham EC, Burks AW, et al. (2002) Protein structure plays a critical role in peanut allergen stability and may determine immunodominant IgE-binding epitopes. J Immunol 169: 882-887.
8. Mueller GA, Maleki SJ, Pedersen LC (2014) The molecular basis of peanut allergy. Curr Allergy Asthma Rep 14: 429.
9. Shin DS, Compadre CM, Maleki SJ, Kopper RA, Sampson H, et al. (2009) J. Biol. Chem. 273, 13573-13759.
10. Pomés A, Vinton R, Chapman MD (2004) Peanut allergen (Ara h 1) detection in foods containing chocolate. J Food Prot 67: 793-798.
11. Wen HW, Borejsza-Wysocki W, DeCoroy TR, Durst RA (2007) Compr. Rev. Food. Sci. F. 6, 47-58.
12. Huang Y, Bell MC, Suni II (2008) Impedance biosensor for peanut protein Ara h 1. Anal Chem 80: 9157-9161.
13. Pollet J, Delport F, Janssen KP, Tran DT, Wouters J, et al. (2011) Fast and accurate peanut allergen detection with nanobead enhanced optical fiber SPR biosensor. Talanta 83: 1436-1441.
14. Careri M, Elviri L, Mangia A, Mucchino C (2007) ICP-MS as a novel detection system for quantitative element-tagged immunoassay of hidden peanut allergens in foods. Anal Bioanal Chem 387: 1851-1854.
15. Gutteridge A, Thornton JM (2005) Understanding nature's catalytic toolkit. Trends Biochem Sci 30: 622-629.
16. Brody EN, Gold L (2000) Aptamers as therapeutic and diagnostic agents. J Biotechnol 74: 5-13.

17. Fang X, Tan W (2010) Aptamers generated from cell-SELEX for molecular medicine: a chemical biology approach. Acc Chem Res 43: 48-57.

18. Wang R, Zhao J, Jiang T, Kwon YM, Lu H, et al. (2013) Selection and characterization of DNA aptamers for use in detection of avian influenza virus H5N1. J Virol Methods 189: 362-369.

19. Lee JF, Hesselberth JR, Meyers LA, Ellington AD (2004) Aptamer database. Nucleic Acids Res 32: D95-100.

20. Martell RE, Nevins JR, Sullenger BA (2002) Optimizing aptamer activity for gene therapy applications using expression cassette SELEX. Mol Ther 6: 30-34.

21. Tran DT, Knez K, Janssen KP, Pollet J, Spasic D, et al. (2013) Selection of aptamers against Ara h 1 protein for FO-SPR biosensing of peanut allergens in food matrices. Biosens Bioelectron 43: 245-251.

22. Pérez-Ruiz E, Kemper M, Spasic D, Gils A, van Ijzendoorn LJ, et al. (2014) Probing the force-induced dissociation of aptamer-protein complexes. Anal Chem 86: 3084-3091.

23. Broeders J, Croux D, Peeters M, Beyens T, Duchateau S, et al. (2013) IEEE Sensors J. 13, 2659-2665.

24. Croux D, Vangerven T, Broeders J, Boutsen J, Peeters M, et al. (2013) Phys. Status Solidi A. 210, 938-944.

25. van Grinsven B, Vandenryt T, Duchateau S, Gaulke A, Grieten L, et al. (2010) Phys. Status Solidi A. 207, 919-923.

26. Christiaens P, Vermeeren V, Wenmackers S, Daenen M, Haenen K, et al. (2006) EDC-mediated DNA attachment to nanocrystalline CVD diamond films. Biosens Bioelectron 22: 170-177 (26).

27. Vermeeren V, Wenmackers S, Daenen M, Haenen K, Williams OA, et al. (2008) Langmuir 24, 9125-9134.

28. Zuker M (2003) Mfold web server for nucleic acid folding and hybridization prediction. Nucleic Acids Res 31: 3406-3415.

29. Tran DT, Vermeeren V, Grieten L, Wenmackers S, Wagner P, et al. (2011) Nanocrystalline diamond impedimetric aptasensor for the label-free detection of human IgE. Biosens Bioelectron 26: 2987-2993.

30. van Grinsven B, Vanden Bon N, Strauven H, Grieten L, Murib M, et al. (2012) Heat-transfer resistance at solid-liquid interfaces: a tool for the detection of single-nucleotide polymorphisms in DNA. ACS Nano 6: 2712-2721.

31. Peeters M, Troost FJ, van Grinsven B, Horemans F, Alenus J, et al. (2012) Sens. Actuators, B: Chemical. 171, 602-610 .

32. Peeters M, Troost FJ, Mingels RH, Welsch T, van Grinsven B, et al. (2013) Impedimetric detection of histamine in bowel fluids using synthetic receptors with pH-optimized binding characteristics. Anal Chem 85: 1475-1483.

33. Wilcoxon J, Schurr JM (1983) Temperature dependence of the dynamic light scattering of linear phi 29 DNA: implications for spontaneous opening of the double-helix. Biopolymers 22: 2273-2321.

34. Erickson HP (2009) Size and shape of protein molecules at the nanometer level determined by sedimentation, gel filtration, and electron microscopy. Biol Proced Online 11: 32-51.

35. Saroff HA, Minton AP (1972) The Hill plot and the energy of interaction in hemoglobin. Science 175: 1253-1255.

Citation: Peeters M, Jiménez-Monroy K, Libert C, Eurlings Y, Cuypers W, et al. (2014) Real-Time Monitoring of Aptamer Functionalization and Detection of Ara H 1 by Electrochemical Impedance Spectroscopy and Dissipation-Mode Quartz Crystal Microbalance. J Biosens Bioelectron 5: 155. doi: 10.4172/2155-6210.1000155